Molecular Therapy
Oncolytics
Original Article

USP18 and USP20 restrict oHSV-1 replication in resistant human oral squamous carcinoma cell line SCC9 and affect the viability of SCC9 cells

Ruitao Lu,[1,3,4] Guangxian Wu,[1,4] Meiling Chen,[1] Dongmei Ji,[2] Yonghong Liu,[1] Grace Guoying Zhou,[3] and Wenmin Fu[3]

[1]School of Basic Medical Sciences, Guangzhou Medical University, Guangzhou 511436, Guangdong, China; [2]Shanghai Cancer Center and Shanghai Medical College, Fudan University, Shanghai 200032, China; [3]Shenzhen International Institute for Biomedical Research, Longhua District, Shenzhen 518116, Guangdong, China

In this study, we discovered that two human oral squamous carcinoma cell (OSCC) lines, SCC9 and SCC25, exhibited varied levels of permissivity to oncolytic HSV-1 T1012G replication and the differential virus yields may associate with the constitutive accumulation of two deubiquitinating enzymes USP18 and USP20 in tumor cells. USP18 and USP20 belong to the ubiquitin-specific protease family, mediating the deubiquitination of targets and promoting antiviral responses. Depletion of USP18 or USP20 in SCC9 cells increased T1012G virus yields; overexpression of USP18 or USP20 in SCC25 cells down-regulated T1012G virus replication. In addition, STING as a verified substrate of USP18 and USP20, was found to affect the virus multiplication of T1012G in SCC9 cells. STING knockdown led to an increase in T1012G virus yields in SCC9 cells. Besides, we introduced a deubiquitinating enzyme inhibitor GSK2643943A targeting USP20 and evaluated its effects on viral replication and tumor killing *in vitro* and *in vivo*. The results showed that the combination of GSK2643934A and T1012G treatment brought a profound anti-tumor efficacy in mice bearing SCC9 tumors. This report explored factors that play roles in mediating oHSV-1 replication in OSCC tumor cells, facilitating to offer potential targets to improve oHSV-1 oncolytic efficacy and develop candidates of biomarkers to predict the efficiency of oHSV-1 multiplication in tumors.

INTRODUCTION

Oral squamous cell carcinoma (OSCC) is the most common oral cancer with a high incidence of metastasis in the head and neck.[1,2] Although the advances in available treatments including surgery, radiotherapy, and chemotherapy, they still present serious side effects and unsatisfactory prognosis. Oncolytic virotherapy (OV) has been widely investigated in clinical trials as a hot alternative to current traditional therapies for various cancer treatments,[3] including OSCC. OV is known to utilize attenuated virus to selectively replicate in and lyse tumor cells, stimulating a systemic immune response to achieve anti-tumor efficacy. Deficient production of virus progeny diminishes the activation of immune responses and death of tumor cells. Thus, efficient multiplication of oncolytic virus inoculum in the tumor cells is crucial to implement the destruction of tumors. However, increasing studies reported that many tumor cell lines exhibited differential susceptibility to oncolytic virus infection[4] and the susceptibility correlates with the cellular antiviral response.[5–8] Oncolytic virus, as an invader, could be recognized by host DNA/RNA sensors and induces innate immune responses defending external invasion.[5,9] Hence, regulation of cellular antiviral response is essential to sufficient virus multiplication in tumor cells.

Deubiquitinating enzymes (DUBs) are known to maintain the ubiquitin system homeostasis by maintaining the balance between deubiquitination and ubiquitination of targets, which have demonstrated their important roles in the innate antiviral immune response. For example, USP3, USP21, and CYLD have been reported to negatively regulate the activation of RIG-I and MDA5 by binding and cleaving the poly-ubiquitin chains.[10–12] USP20 removes ubiquitin chains from stimulator of interferon genes (STING) after HSV-1 infection to stabilize STING, promoting cellular antiviral responses.[13]

Since DUBs act as key mediators between the virus and its host, in this study, we explored the potential functions of DUBs (USP18 and USP20) in mediating the susceptibility of tumor cells to oncolytic herpes simplex virus 1 (oHSV-1) infection. Two OSCC cell lines, SCC9 and SCC25, which present varied levels of sensitivity to oHSV-1 infection, as we found in the preliminary study, were applied in this report to investigate the roles that USP18/USP20 play in oHSV-1 productive replication and even oncolytic activity, developing potential combination strategy for anti-tumor treatment and candidates of biomarkers that could predict the efficiency of oHSV-1 multiplication in tumors.

Received 25 January 2021; accepted 7 November 2021;
https://doi.org/10.1016/j.omto.2021.11.004.

[4]These authors contributed equally

Correspondence: Wenmin Fu, Shenzhen International Institute for Biomedical Research, Longhua District, Shenzhen 518116, Guangdong, China.
E-mail: Wenmin.Fu@siitm.org.cn
Correspondence: Grace Guoying Zhou, Shenzhen International Institute for Biomedical Research, Longhua District, Shenzhen 518116, Guangdong, China.
E-mail: zhoug@siitm.org.cn

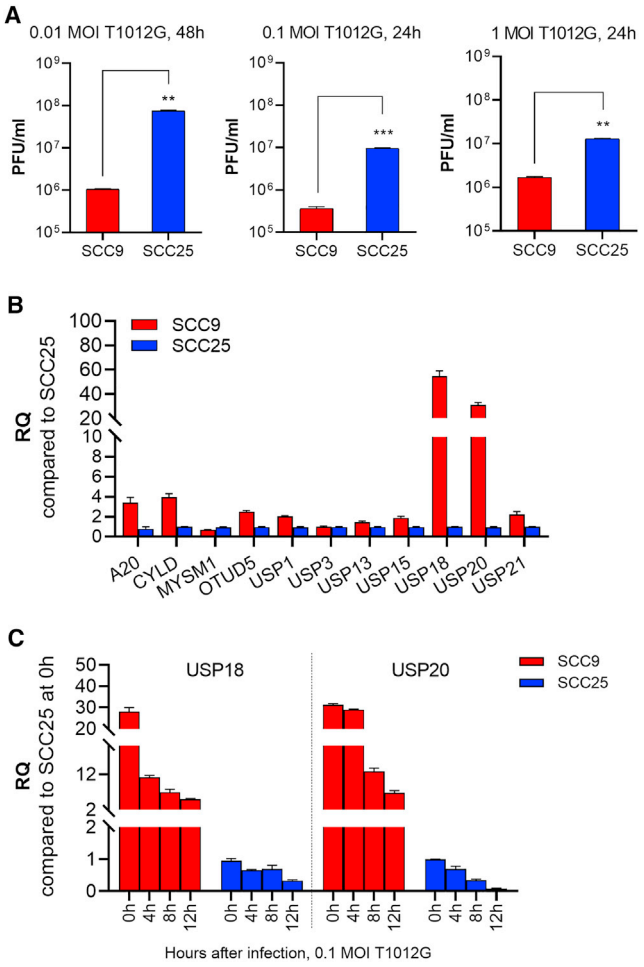

Figure 1. mRNA accumulation of indicated deubiquitinating enzymes in human tongue squamous carcinoma cells SCC9 and SCC25

(A) Viral production of oHSV-1 T1012G in human tongue squamous carcinoma cells SCC9 and SCC25. (B) Constitutive accumulation of selected DUB mRNA in SCC9 and SCC25 cells. (C) Accumulation of USP18 and USP20 mRNA in oHSV-1 T1012G-infected SCC9 and SCC25 cells. Error bar, mean ± SEM.

RESULTS

Two human OSCC lines, SCC9 and SCC25, exhibited varied levels of sensitivity to oHSV-1 T1012G infection. SCC9 and SCC25 were evaluated for their susceptibility to oHSV-1 T1012G infection. T1012G has been described elsewhere in which the inverted repeats of HSV-1 viral genome were replaced by sequences encoding the cytomegalovirus (CMV) promoter followed by three stop codons.[14] T1012G is an attenuated HSV-1 without foreign genes inserted, which was used as the backbone to develop new generations of oHSV-1. We infected these two cell lines with T1012G at a multiplicity of infection (MOI) of 0.01, 0.1, and 1 infectious virus particle per cell. Cells were harvested for the examination of virus titer at 24 or 48 h post-infection. As shown in Figure 1A, SCC9 cells had less virus multiplication than SCC25 cells, regardless of the dose of virus inoculum. This indicates that cell line SCC9 presents low permissivity to oHSV-1 T1012G infection. Thus, we defined SCC9 as an oHSV-1-resistant cell line, and SCC25 as an oHSV-1-sensitive cell line, according to the amount of T1012G virus yields. Subsequently, these two cell lines were applied for more examination to explore the mechanism of how tumors from the same origin possess varied sensitivities to oHSV-1 replication.

Constitutively higher mRNA accumulation of USP18 and USP20 in SCC9 cells

DUBs are a group of proteases that remove ubiquitin from target substrates and play roles in regulating antiviral immune responses.[15] In order to explore the possible functions of DUBs that correlate with limited virus yields in SCC9 cells, we examined the intrinsic mRNA accumulation of some "signature" DUBs in SCC9 and SCC25 cells, such as *A20*, *CYLD*, *MYSM1*, *OTUD5*, *USP1*, *USP3*, *USP13*, *USP15*, *USP18*, *USP20,* and *USP21*, which have exhibited their association with virus-induced immune response.[10–12,15,16] We found that USP18 and USP20 have remarkably high levels of mRNA accumulation in SCC9 cells among these DUBs when compared with those in SCC25 cells (Figure 1B). Besides, upon exposure to oHSV-1 T1012G infection, although USP18 and USP20 mRNA accumulation was dynamically changed for responding to foreign invasion, the overall levels of USP18 and USP20 mRNA in SCC9 cells were apparently higher than those in SCC25 cells (Figure 1C). Therefore, we hypothesized that abundant USP18 and USP20 accumulation limits the ability of oHSV-1 T1012G replicating in SCC9 cells.

Depletion of USP18 or USP20 enhanced oHSV-1 T1012G lytic replication in SCC9 cells

To verify the above hypothesis, we investigated the effects of USP18 and USP20 genetic depletion on T1012G virus yields in SCC9 cells. Small interfering RNA (siRNA)-mediated knockdown of USP18 and USP20 was performed in SCC9 cells (Figure 2A). USP18- and USP20-depleted SCC9 cells subsequently were exposed to 0.01 and 0.1 MOI T1012G virus infection. Virus progeny were harvested and virus titers were examined using the plaque assay. As shown in Figure 2B, USP18 and USP20 knockdown visibly increased virus yields of T1012G in SCC9 cells when compared with mock depletion. Besides, western blotting was performed to confirm USP18/USP20 knockdown and analyze the expression of viral proteins in USP18- or USP20-depleted SCC9 cells upon 5 MOI T1012G infection. As shown in Figures 2C and 2E, specific siRNA transfection brought efficient knockdown of USP18 and USP20 protein expression, and depletion of USP18/USP20 led to general increases of viral proteins in SCC9 cells. Besides, we examined the transcript levels of viral genes ICP8 and VP16 in SCC9 cells when USP18 or USP20 was depleted. As shown in Figures 2D and 2F, either USP18 knockdown or USP20 knockdown increased viral mRNA accumulation in SCC9 cells. These results showed USP18 or USP20 knockdown increased virus replication in SCC9 cells, which is consistent with the hypothesis, suggesting that USP18 and USP20 may act as a restricting factor to limit the lytic replication of oHSV-1 T1012G in SCC9 cells.

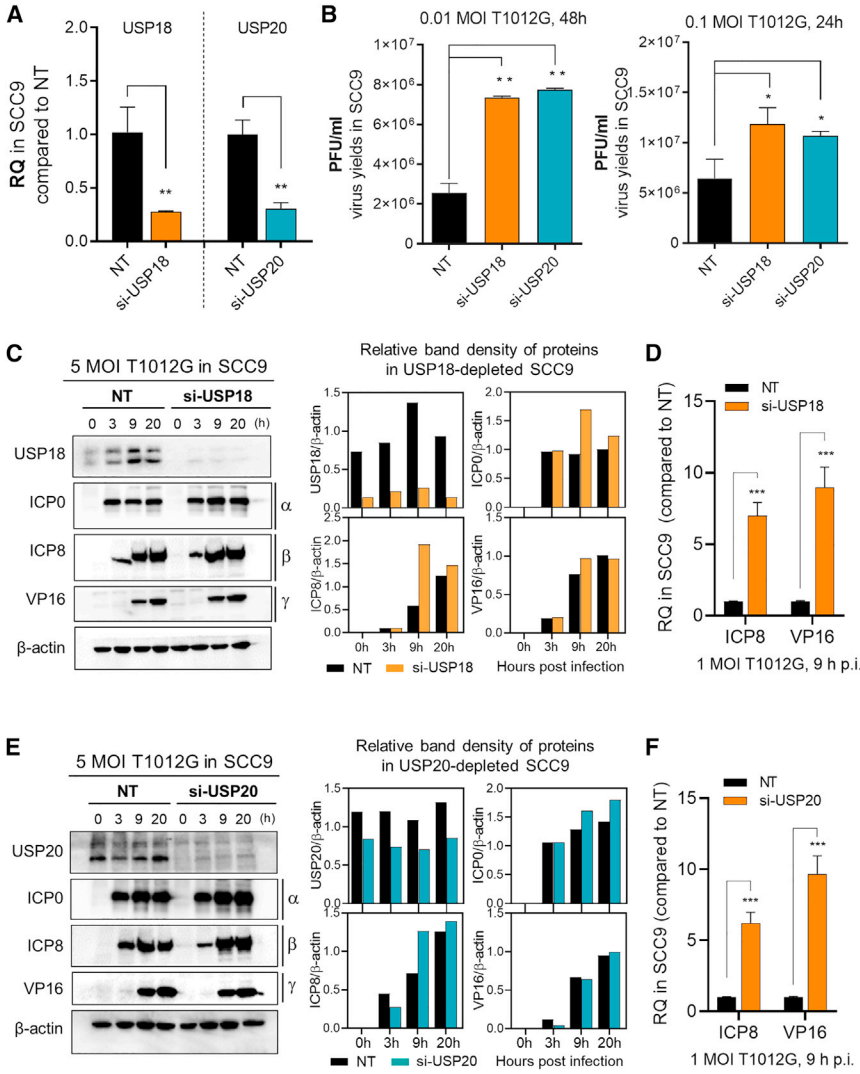

Figure 2. Effects of USP18 and USP20 depletion on viral lytic replication in SCC9 cells

(A) Examination of si-USP18 and si-USP20 knockdown efficiency. Error bar, mean ± SEM. (B) Virus yields in USP18 or USP20-depleted SCC9 cells. (C and E) Accumulation of viral proteins in USP18 or USP20-depleted SCC9 cells. β-actin serves as a loading control. In addition, the band density of viral protein by gray analysis. Relative density was normalized to β-actin. (D and F) mRNA accumulation levels of viral ICP8 and VP16 in SCC9 cells.

Identification of interactions among USP18, USP20, and STING in SCC9 cells

STING is well known to mediate the innate antiviral signaling, and was identified as the substrate of USP18 and USP20.[5,17,18] Zhang et al. have reported that USP18 recruits USP20 to deconjugate the ubiquitination of STING, which promotes the production of type I interferons after DNA virus infection.[13,19] Here we assumed that USP18 and USP20 boost antiviral responses through stabilizing STING in SCC9 cells, which leads to limited oHSV-1 T1012G virus yields. To verify the assumption, we first examined the association among USP18, USP20, and STING in SCC9 cells. We performed co-immunoprecipitation and immunoblot assays to identify if USP18 and USP20 are STING-interacting proteins in interferon (IFN)β-activated SCC9 cells. We found that USP18 and USP20 both interact with STING in SCC9 cells. IN addition, there existed a protein association between USP18 and USP20 (Figure 4A), consistent with previously described USP18-mediated recruitment of USP20.[19] Next, we explored the influences of USP18 or USP20 depletion on STING protein levels in SCC9 cells. Cycloheximide (CHX; 100 μg/mL) was used to block protein synthesis for better investigating the degradation of STING in USP18- or USP20-depleted SCC9 cells. As shown in Figure 4B, the knockdown of USP18 and USP20 both led to a notable reduction of STING protein levels in SCC9 cells. Collectively, these results showed that USP18 and USP20 interact with STING and that a deficiency of either USP18 or USP20 affects the stability of STING in SCC9 cells.

Overexpression of USP18 or USP20 down-regulated oHSV-1 T1012G lytic replication in SCC25 cells

The gain-of-function experiments were performed to investigate the effects of USP18 and USP20 on T1012G virus yields in SCC25 cells. As shown in Figure 3A, plasmid transfection of P-USP18 and P-USP20 led to significant increases of mRNA accumulation and protein expression in SCC25 cells when compared with empty plasmid pEn-CMV-neo transfection. Plasmid-expressed USP18 and USP20 both led to 50% decreases in virus yields in SCC25 cells (Figure 3B). Moreover, western blotting was performed to examine viral protein ICP8 levels. Protein and mRNA levels of ICP8 were slightly decreased in USP18-overexpressed and USP20-overexpressed SCC25 cells (Figures 3C and 3D). These results suggest that USP18 and USP20 affect the permissivity of SCC9 and SCC25 cells to oHSV-1 T1012G replication.

Altered STING accumulation influenced oHSV-1 T1012G lytic replication in SCC9 cells

Based upon the above-described results, we hypothesized that STING function relates to oHSV-1 resistance in SCC9 cells and (1) genetic depletion of STING in SCC9 cells could enhance levels of oHSV-1 T1012G replication; and (2) overexpression of STING in SCC25 cells could decrease oHSV-1 T1012G virus yields. To

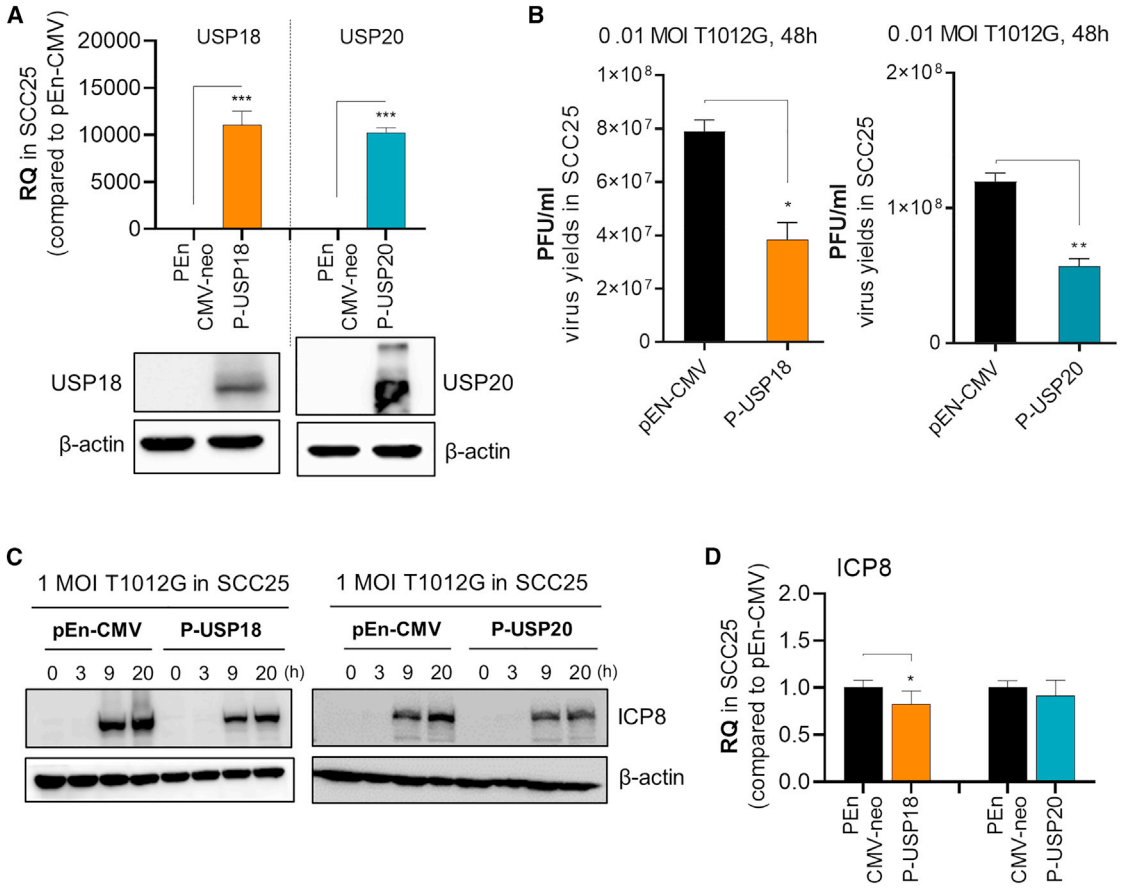

Figure 3. Effects of USP18 and USP20 overexpression on viral lytic replication in SCC25 cells

(A) Examination of USP18 and USP20 plasmid transfection efficiency. Error bar, mean ± SEM. (B) Virus yields in USP18 or USP20-overexpressed SCC25 cells. (C) Accumulation of viral protein ICP8 in USP18 or USP20-depleted SCC5 cells. β-actin serves as a loading control. (D) Examination of viral mRNA levels in USP18- or USP20-overexpressed SCC25 cells.

prove this, we first performed an siRNA-mediated knockdown of STING in SCC9 cells. mRNA levels of STING in SCC9 cells were analyzed via RT-qPCR assay. Si-STING transfection led to significant reduction in STING mRNA levels in SCC9 cells (Figure 4C). Upon 0.01 MOI and 0.1 MOI oHSV-1 T1012G infection, STING depletion led to a visible increase in virus yields in SCC9 cells (Figure 4D). We also examined the effect of STING overexpression on oHSV-1 T1012G virus titers in SCC25 cells. As shown in Figure 4E, STING plasmid transfection remarkably increased STING mRNA accumulation in SCC25 cells when compared with empty plasmid pcDNA3.1 transfection. And plasmid-expressed STING resulted in almost 50% loss of virus yields in SCC25 cells (Figure 4F).

Taken together, these results showed that altered STING accumulation affects oHSV-1 T1012G virus production in SCC9 and SCC25 cells, suggesting that STING as a substrate of USP18 and USP20, suppressing the ability of oHSV-1 to replicate in SCC9 cells.

USP20 inhibitor GSK2643943A influences oHSV-1 T1012G productive infection in SCC9 cells

Our above results demonstrated that (1) USP18 and USP20 correlate with limited oHSV-1 T1012G virus yields in SCC9 cells; (2) USP18 and USP20 interact with STING and alter the levels of STING proteins in SCC9 cells; and (3) altered STING accumulation regulates viral replication in SCC9 and SCC25 cells, while we need to further examine whether the DUB activity of USP18 or USP20 is crucial for the regulation of STING stabilization and oHSV-1 T1012G virus replication. We introduced GSK2643943A (GSK), which is a DUB inhibitor targeting USP20 to evaluate the influences of the DUB activity on viral replication in SCC9 cells. First, we examined the inhibitory efficiency of GSK on deubiquitination in SCC9 cells through the detection of Ub and STING protein levels using co-immunoprecipitation (Co-IP) assay. As shown in Figure 5A, GSK treatment resulted in increased protein accumulation of Ub and slightly decreased STING protein in SCC9 cells when compared with the DMSO mock-treated group. These indicate that GSK blocked the USP20-mediated cleavage of protein-ubiquitin bonds. Then, we

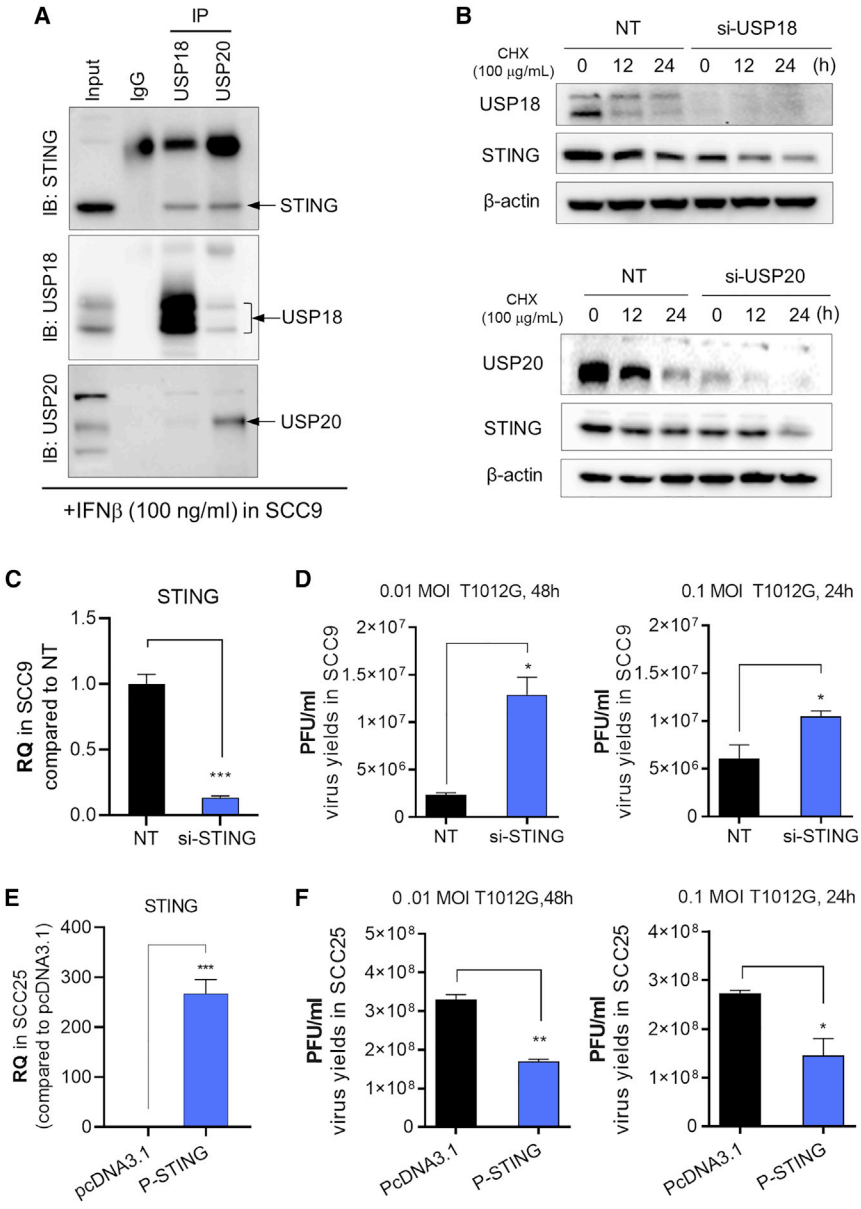

Figure 4. STING interacts with USP18 and USP20 in SCC9 cells and affects oHSV-1 T1012G virus yields

(A) Verification of protein interactions among USP18, USP20, and STING in SCC9 cells via Co-IP assay. (B) USP18/USP20 depletion affects STING protein levels in SCC9 cells. (C) Examination of si-STING knockdown efficiency in SCC9 cells. (D) Virus yields in STING-depleted SCC9 cells. (E) Examination of STING plasmid transfection efficiency. (F) Virus yields in STING-overexpressed SCC25 cells.

investigated the effects of GSK treatment on T1012G virus titer in SCC9 cells. As shown in Figure 5B, GSK (1 μM) treatment led to a notable increase of virus yields in SCC9 with 0.01 MOI and 0.1 MOI T1012G infection. Besides, viral protein expression and mRNA levels were examined. The expression of viral proteins at various phases was generally up-regulated (Figure 5C) and the accumulation of viral ICP8 and VP16 mRNA was significantly increased (Figure 5D) by GSK treatment in SCC9 cells. All these results suggest that the DUB activity is indispensable for limited virus multiplication in SCC9 cells and USP18/USP20 regulates the ubiquitination levels of STING to affect the accumulation of STING protein and the production of antiviral signaling. USP18-USP20 mediated the accumulation of STING that regulates oHSV-1 T1012G viral lytic replication in SCC9 cells.

As we have shown above that GSK treatment enhanced oHSV-1 T1012G replication in SCC9 cells, here we further investigated whether GSK treatment could promote virus-induced loss of SCC9 viability. Cell viability of SCC9 cells was determined by CCK-8 assay kit under T1012G infection at a different dose and GSK treatment with different concentrations: 5 μM GSK treatment displayed a significant drop in viability ($\geq$50%) with 0.01 MOI T1012G infection, and 1 μM GSK treatment together with 0.1 MOI T1012G infection caused 50% loss of SCC9 viability (Figure 5E). Upon exposure to 1 MOI T1012G infection, GSK treatment brought a remarkable reduction in the viability of SCC9 (Figure 5F). These results suggest that GSK treatment renders SCC9 cells more susceptible to oHSV-1 induced oncolysis.

The evaluation of the anti-tumor effects of GSK and oHSV-1 T1012G combined treatment in SCC9 tumors

We demonstrated the influences of GSK and oHSV-1 T1012G combined treatment on SCC9 cell-killing *in vitro*, next we investigated the effects of GSK-T1012G combined treatment on tumor suppression *in vivo*. Nude BALB/c mice were injected with SCC9 cells to induce tumor growth. Once the tumor volume reached 70 to 120 mm^3, the mice were randomized into four groups (n = 7, per group) for evaluating the anti-tumor efficacy of various treatments. The condition of treatments is shown in Figure 6A. (1) Vehicle: intratumoral injection with 50 μL of PBS; (2) GSK2643943A: intraperitoneal administration with GSK2643943A (5 mg/kg) daily for 6 days; (3) T1012G: intratumoral injection with 50 μL of 1 × 10^6 PFU T1012G in PBS on day 1, day 4, and day 7; and (4) Combination: intraperitoneal administration with GSK2643943A (5 mg/kg) daily for 6 days, intratumoral injection with 50 μL of 1 × 10^6 PFU T1012G in PBS on day 1, day 4, and day 7. Tumor sizes were

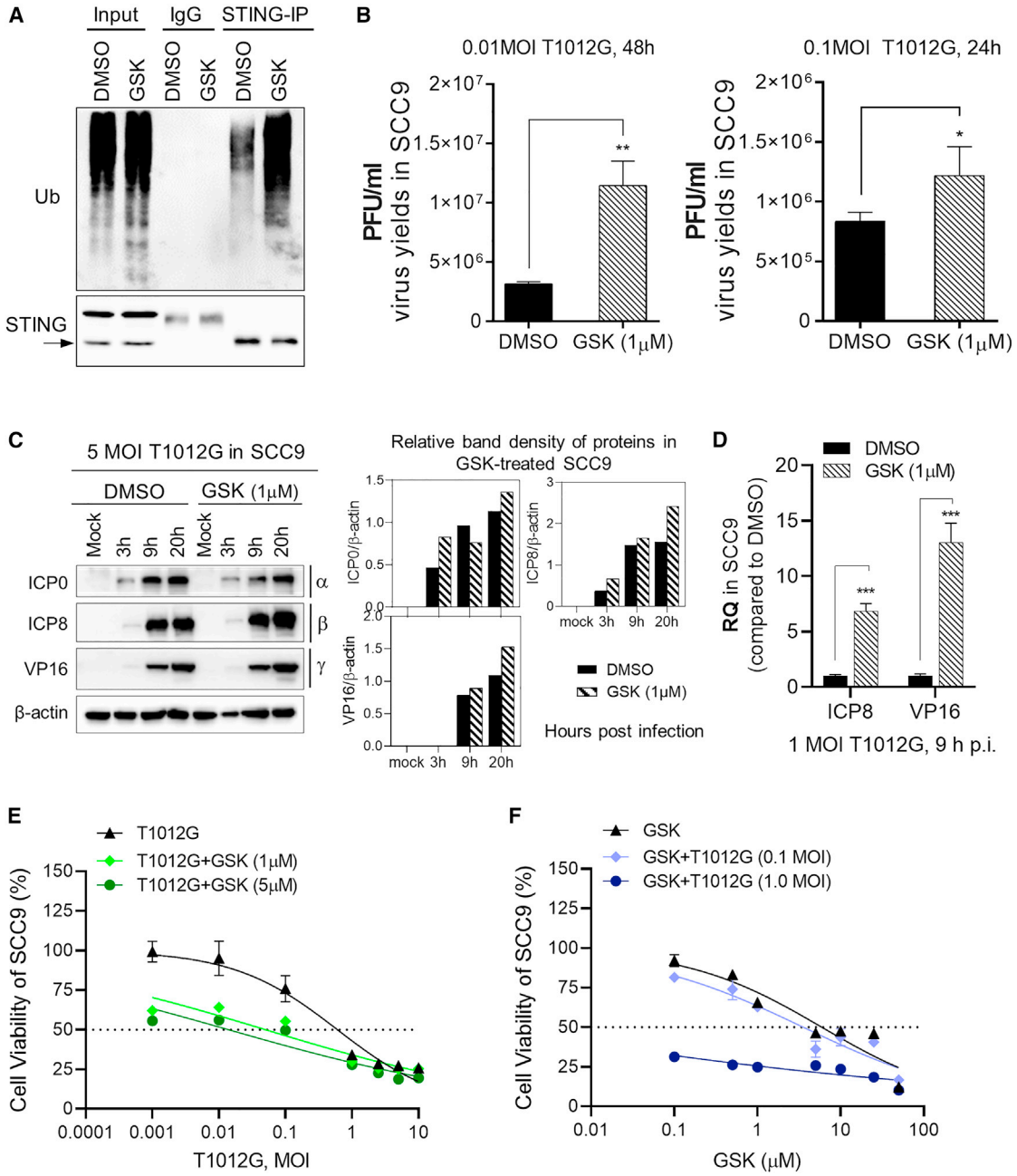

Figure 5. USP20 inhibitor GSK2643943A influences oHSV-1 T1012G productive infection and viability in SCC9 cells

(B) Co-IP analysis of poly-ubiquitin, STING, and β-actin in SCC9 cells. (B) Virus yields in GSK-treated SCC9 cells under 0.01 MOI or 0.1 MOI T1012G infection. (C) Accumulation of viral proteins in SCC9 cells infected with 5MOI T1012G for 0 to 20 h in the presence of GSK (1 μM). β-actin serves as a loading control. Relative density was calculated by gray analysis and normalized to β-actin. (D) mRNA accumulation levels of viral ICP8 and VP16 in GSK-treated SCC9 cells. (E, F) Cell viability of SCC9 cells was determined by CCK-8 assay kit under T1012G infection at a different dose and GSK treatment with different concentrations.

measured by length and width every 2 days for 25 days. The average tumor volume of SCC9 tumors under various treatments was calculated and compared as shown in Figure 6B. The reduction in tumor volumes was the most significant in mice with combined treatment of GSK and oHSV-1 T1012G. Although the solo treatment of GSK or T1012G caused a visible drop of tumor volumes when compared with the PBS mock treatment, it is incontestable that GSK treatment boosted the anti-tumor effects of oHSV-1 T1012G. All mice were killed on day 25 after treatment, tumors were resected and weighed as shown in Figure 6C. Viral mRNA levels were examined in SCC9

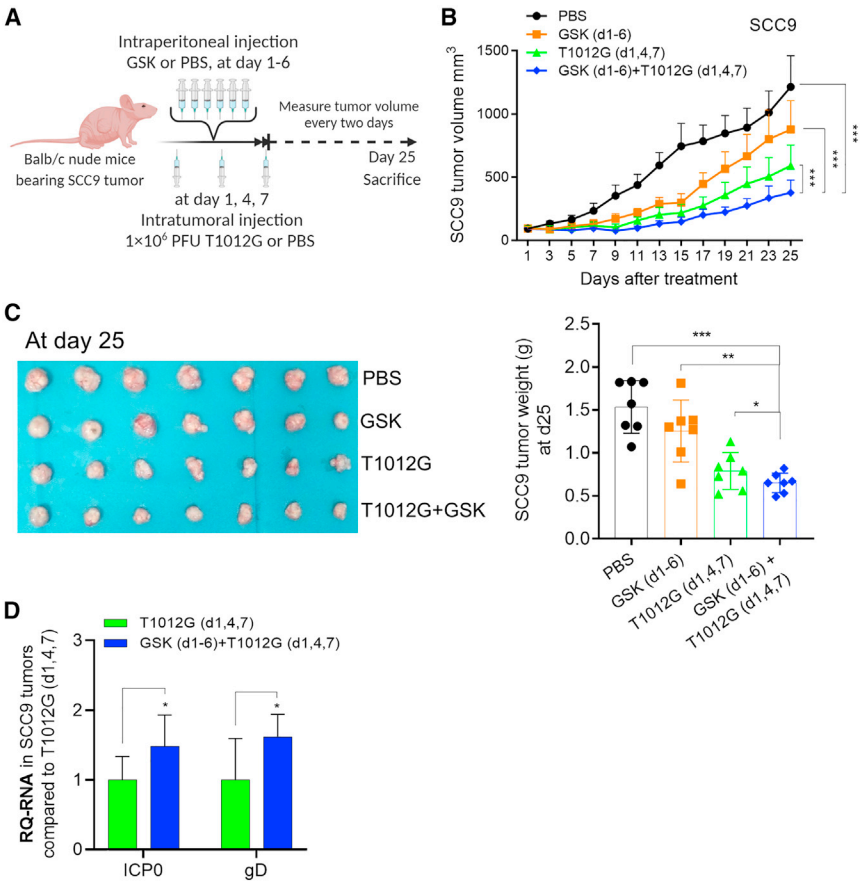

Figure 6. The cell viability and anti-tumor efficacy of combined treatment of oHSV-1 T1012G and GSK in SCC9 tumors

(A) Experimental design of the study in mice, as detailed in the text. (B) The growth of SCC9 tumors in mice treated by PBS, T1012G, GSK, or combination treatment. Tumor volume was examined every other day for 25 days and calculated by the formula: length × width^2 × 0.5. Data are mean ± SEM, n = 7 in each group. ***p < 0.001. (C) Examination of tumor weight at day 25 after treatment. SCC9 tumors were excised and photographed on day 25 after treatment. (D) Examination of viral mRNA levels in SCC9 tumors.

tumors at 48 h post first T1012G administration via qPCR assay. As shown in Figure 6D, GSK treatment in SCC9 tumors brought a slight increase in viral ICP0 and gD mRNA accumulation. Consistent with the above results, the combination of GSK and T1012G treatment exhibited a profound anti-tumor effect. To sum up, GSK treatment potentiated oHSV-1-induced oncolysis in SCC9 tumors.

The evaluation of the effects of USP18, USP20, and GSK in oHSV-1 T1012G replication and oncolytic activity in SCC7 cells and tumors

A parallel experiment was performed in a mouse OSCC (SCC7). As shown in Figure 7A, we tested the knockdown efficiency of mouse si-USP18 and si-USP20 in SCC7 cells. The virus yields of oHSV-1 T1012G, viral protein expression, and viral mRNA levels were examined in USP18- or USP20-depleted SCC7 cells. The data showed that USP18 or USP20 knockdown led to notable increases of virus titer in SCC7 cells (Figure 7B). Protein and mRNA levels of ICP8 and VP16 were up-regulated by USP18 or USP20 depletion in SCC7 cells (Figures 7C and 7D). Besides, the effect of GSK treatment on oHSV-1 T1012G multiplication in SCC7 cells was also investigated. As shown in Figure 7E , GSK (1 μM) treatment led to a notable increase of virus yields in SCC9 with 0.01 MOI infection.

Moreover, we demonstrated the influences of GSK and oHSV-1 combined treatment on SCC7 tumor suppression *in vivo*. Different from the SCC9 mouse model, the SCC7 mouse model is immune-competent. The design of treatments as follows: (1) Vehicle: intratumoral injection with 50 μL of PBS; (2) GSK2643943A: intraperitoneal administration with GSK2643943A (2.5 mg/kg) daily for 9 days; (3) T1012G: intratumoral injection with 50 μL of 1 × 10^7 PFU T1012G in PBS on days 1, 4, 7, and 10; and (4) Combination: intraperitoneal administration with GSK2643943A (2.5 mg/kg) daily for 9 days, intratumoral injection with 50 μL of 1 × 10^7 PFU T1012G in PBS on days 1, 4, 7, and 10. Tumor sizes were measured by length and width every 2 to 3 days for 19 days. The average tumor volume of SCC9 tumors under various treatments was calculated and compared as shown in Figure 7F. The reduction in tumor volumes was the most significant in mice with combined treatment of GSK and oHSV-1 T1012G. Although the solo treatment of GSK or T1012G caused a visible drop of tumor volumes when compared with the PBS mock treatment, it is incontestable that GSK treatment boosted the anti-tumor effects of oHSV-1 T1012G, which is consistent with the observation in the SCC9 mouse study. Viral mRNA levels were examined in SCC7 tumors at 48 h post first T1012G administration via qPCR assay. As shown in Figure 7G, GSK treatment in SCC7 tumors brought a slight increase in viral ICP0 and gD mRNA accumulation. These above all indicate the regulatory roles that USP18, USP20, and GSK play in oHSV-1 T1012G replication and oncolysis in SCC7 cells.

DISCUSSION

Oncolytic virus strategies for anti-tumor therapy has attracted attention for decades and emerged as a hot alternative to radiotherapy and chemotherapy for various cancer treatments. However, like other therapeutic strategies, oncolytic virus has its own challenges, like antiviral immune responses. Upon the oncolytic virus infection, tumor cells immediately initiate the innate antiviral response, which causes a harsh environment for virus lytic replication, the virus production might be repressed at a certain extent, correspondingly the inefficient

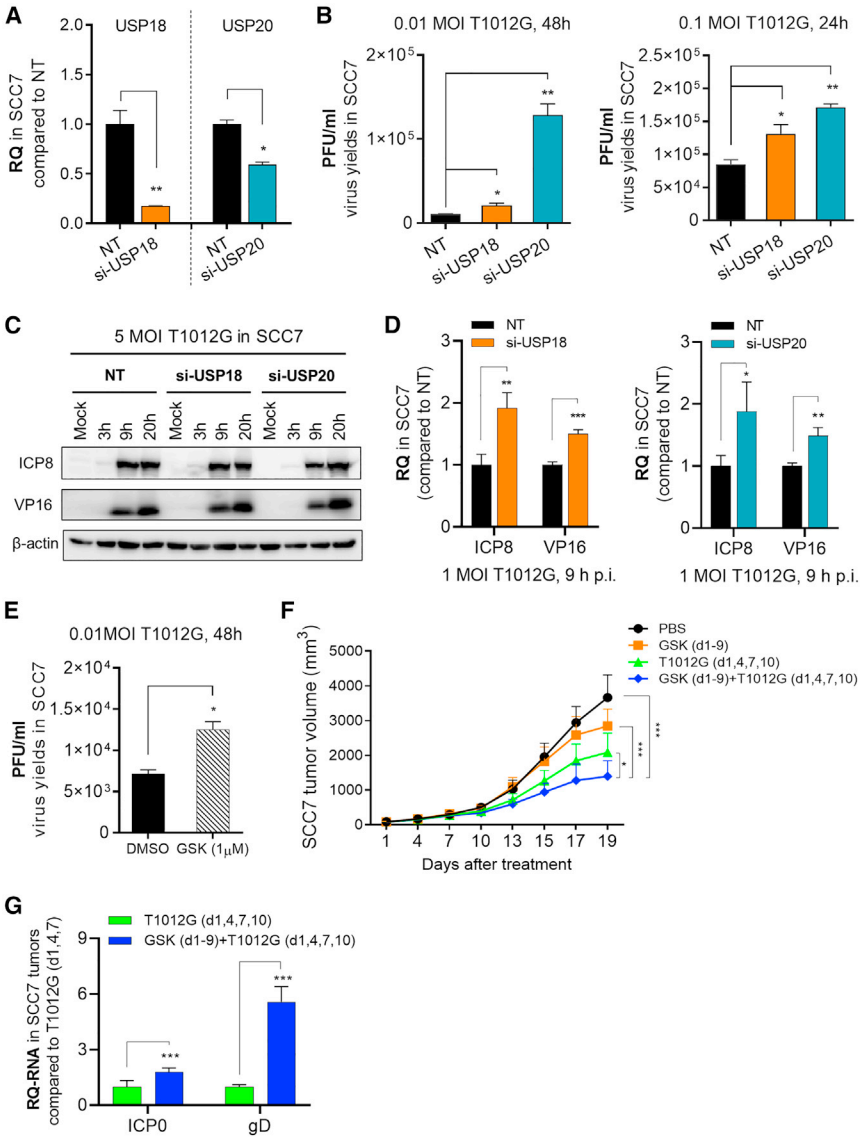

Figure 7. Effects of USP18, USP20, and GSK on oHSV-1 T1012G replication and oncolytic activity in SCC7 cells and tumors

(A) Examination of mouse si-USP18 and si-USP20 knockdown efficiency. Error bar, mean ± SEM. (B) Virus yields in USP18- or USP20-depleted SCC7 cells. (C) Accumulation of viral proteins in USP18- or USP20-depleted SCC7 cells. β-actin serves as a loading control. (D) mRNA accumulation levels of viral ICP8 and VP16 in SCC7 cells. (E) Virus yields in GSK-treated SCC7 cells under 0.01 MOI T1012G infection. (F) The growth of SCC7 tumors in mice treated by PBS, T1012G, GSK, or combination treatment. (G) Examination of viral mRNA levels in SCC7 tumors.

tumor oncolysis as well. Therefore, increasing studies investigated the interplay among the oncolytic virus, tumor cells, and innate immune factors to explore the potential mechanisms or develop more potential targets for improving the oncolytic activity of virus.

DUBs are a group of proteases that counteract the activity of ubiquitin ligase, removing ubiquitin from the target substrates and playing a role in controlling immune responses.[10,11,15] In this report, we evaluated the levels of different DUBs mRNA accumulation in resistant SCC9 and sensitive SCC25 cells to screen potential DUBs that correlate with limited virus reproduction in SCC9 cells. We found USP18 and USP20 were highly expressed in resistant SCC9 cells, and subsequently discovered that depletion of USP18 or USP20 in SCC9 cells was verified to increase oHSV-1 T1012G virus yields, while overexpression of USP18 or USP20 in SCC25 cells reduced oHSV-1 T1012G virus titer. Given these, we demonstrated that USP18 and USP20 affect the permissivity of SCC9 and SCC25 cells to oHSV-1 T1012G replication. In addition, we performed parallel experiments in mouse squamous cell carcinoma SCC7 cells (Figure 7). siRNA-mediated depletion of USP18 or USP20 in SCC7 cells moderately increased oHSV-1 T1012G virus yields, viral mRNA, and protein accumulation.

Subsequently, STING as a substrate of USP18 and USP20 attracted our attention to explore its roles in SCC9 and SCC25 cells. First, we verified the interactions among USP18, USP20 and STING in resistant SCC9 cells. And the levels of STING proteins were reduced when USP18 or USP20 was depleted. STING is a facilitator of innate immune signaling that acts as a sensor of viral DNA and promotes the production of IFNs.[17,18,20] A recent study has reported STING's roles in oHSV resistance that STING could restrict oHSV replication and spread in resistant malignant peripheral nerve sheath tumors (MPNSTs).[8] Similarly, in this study we demonstrated that depletion of STING enhanced oHSV-1 virus replication in resistant oral squamous carcinoma cell line SCC9, overexpression of STING reduced oHSV-1 T1012G virus titer in SCC25 cells. All the above results indicate that USP18-USP20 mediated the accumulation of STING function with limited oHSV-1 T1012G virus yields in SCC9 cells.

Besides, we employed the DUB inhibitor targeting USP20 GSK2643943A (GSK) to evaluate the effects of DUB activity on viral oncolysis of SCC9 tumors *in vitro* and *in vivo*. GSK treatment was shown to bring a remarkable reduction in the viability of SCC9 upon oHSV-1 infection. The combination of GSK and oHSV-1 T1012G treatment led to a significant decrease of SCC9 tumor volumes in mice, similar results were observed in immune-competent

mice bearing SCC7 tumors. These generate a possibility to develop USP20 inhibitor as a co-effector of OV in anti-tumor treatment. It is worth noting that USP20 was reported to positively regulate tumorigenesis and chemoresistance through β-catenin deubiquitination and stabilization.[21] These all broaden our understanding of USP20 as the potential target for anti-tumor strategies and as the potential marker for predicting oHSV-1 resistance and chemoresistance in cancer.

Although we observed the depletion of USP18 likewise decreased the levels of STING protein and improved virus reproduction in resistant SCC9 cells, the further investigation of its effects on tumor oncolysis in tumors was impeded due to the unavailable commercial inhibitor targeting USP18. Similarly, USP18 was also reported to have roles in promoting cancer growth. USP18 was found to promote breast cancer development by upregulating epidermal growth factor receptor (EGFR) and subsequently activating the AKT/Skp2 feedback loop pathway.[16] USP18 depletion improves EGFR expression and the tumorigenic activity of cancer cells via elevating miR-7 levels.[22] As described above, USP18 could be a promising target for anti-tumor treatment. But the questions concerning the promising application of USP18 in anti-tumor therapy remain to be addressed by more investigation in the future.

Meanwhile, USP18 and USP20 demonstrated their potential association with OSCC tumor sensitivity to oHSV-1 replication. Identifying the functions of USP18 and USP20 in a wider panel of tumors and verifying their potentials as biomarker candidates to predict the efficiency and efficacy of oHSV-1 treatment for anti-tumor application would be another subject to be launched in the future.

MATERIALS AND METHODS

Cells, viruses, and reagents

OSCC lines SCC9 and SCC25 were obtained from the BeNa Culture Collection (BNCC, China), SCC7 was gifted from Prof. Bernard Roizman at the University of Chicago. All these cells were cultured in DMEM (Thermo Scientific, USA) supplemented with 10% fetal bovine serum (FBS; Thermo Scientific, USA). Vero (CCL-81) cells were purchased from the American Type Culture Collection (USA) and cultured in DMEM supplemented with 50% newborn calf serum (NBCS; Thermo Scientific, USA). All cell lines were incubated at 37°C in a humidified atmosphere of 5% CO_2. Oncolytic HSV-1 recombinant virus T1012G (oHSV-1 T1012G) was previously described.[14] Immunoglobulin (Ig)G (S20043008) was obtained from the Shenzhen Weiguang Biological Co., Ltd, China. Cycloheximide (HY-12320) and GSK2643943A (HY-111458) were purchased from MedChem Express (MCE, USA).

Virus inoculation and virus titration

SCC9, SCC25, or SCC7 cells seeded in six-well plates were exposed to 0.01 MOI, 0.1 MOI, or 1 MOI - T1012G in serum-free medium for 2 h or 1 h, respectively. The medium was aspirated and replaced with fresh medium supplemented with 10% FBS. For virus titration, virus-containing cells were harvested and lysed with three freeze-and-thaw cycles. The virus titer was measured using the conventional plaque assay. Vero (CCL-81) cells seeded on T25 flask were infected with serial 10-fold-diluted virus suspensions in a duplicate manner and incubated at 37°C, 5% CO_2 for 2 h. Subsequently, cells were washed twice with PBS and incubated with fresh medium with 1% NBCS and 1% IgG for an additional 3 days until visible plaque was detected. Cells were stained with crystal violet and the plaques were counted to calculate the virus yields.

RNA isolation, reverse-transcription, and real-time quantitative PCR

Cells were harvested for total RNA isolation using TRI Reagent solution (Thermo Scientific, USA) followed with DNase I (Takara, Japan) treatment; 0.5 μg total RNA was reverse-transcribed to cDNA with the aid of the Rever Era Ace qPCR RT Kit (TOYOBO, Japan) under the manufacturer's instructions. mRNA accumulation was analyzed by quantitative PCR using SYBR Green Real-time PCR master mix (TOYOBO, Japan) in Step on plus Real-time PCR system (Applied Biosystems, USA) with indicated primers. USP18 primers (F: 5′-GAGCTTGGATTTCAGTCAGGTT-3′; R: 5′-CATTGAAGCAGAACCACTTTCC-3′); USP20 primers (F: 5′-GGCTGATGAAGGAGAGTCTGAG-3′; R: 5′-GCCACACTCCAAGAAGAACTGA-3′); other used primers were described elsewhere.[23] We used 18S as the normalization control. Relative quantity of gene expression was determined with the $2^{-\Delta\Delta Ct}$ method.

siRNA transfection

Genetic depletion was achieved using siRNA targeting human USP18, USP20, or STING genes. All siRNAs were purchased from GenePharma (China) and listed with sequences as follows:

Human si-USP18 (sense: 5′-CUGCAUAUCUUCUGGUUUATT-3′, antisense: 5′-UAAACCAGAAGAUAUGCAGTT-3′);

Human si-USP20 (sense:5′-GCAGCGUCAUCUCAGACAUTT-3′, antisense: 5′-AUGUCUGAGAUGACGCUGCTT-3′);

Human si-STING (sense 5′-GCCCUUCACUUGGAUGCUUTT-3′, antisense: 5′-AAGCAUCCAAGUGAAGGGCTT-3′);

Mouse si-USP18 (sense: 5′-CGUCCAGCCCAAAGAGUUATT-3′, antisense: 5′-UAACUCUUUGGGCUGGACGTT-3′);

Mouse si-USP20 (sense: 5′-GGACCUAACCUAUGGGCUUTT-3′, antisense: 5′-AAGCCCAUAGGUUAGGUCCTT-3′).

The non-target siRNA (NT) (sense: 5′-UUCUCCGAACGUGUCACGUTT-3′) was used as a negative control.

For siRNA transfection, cells (3×10^5 per well) seeded in six-well plates were transfected with siRNA at a final concentration of 30 pmol. All siRNA transfection was carried out using RNAiMAX transfectamine (Invitrogen, USA) according to the manufacturer's protocol.

Plasmid transfection

Plasmids pEnCMV (Cat No. P13305), pEnCMV-USP20 (Cat No. P22486), pEnCMV-USP18 (Cat No. P22489), pcDNA3.1 (Cat No. P0160), and pcDNA3.1-STING (Cat No. P8966) were purchased from MiaoLing Plasmid Sharing Platform, China. Cells seeded in six-well plates were transfected with 1 μg plasmids using Lipofectamine 3000 according to the manufacturer's protocol (Invitrogen, USA).

Western blot analysis

Harvested cells were lysed with RIPA lysis buffer (Beyotime, China) supplemented with 1 mM protease inhibitor PMSF (Beyotime, China). Cells listed were heat-denatured and separated on SDS-containing polyacrylamide gels, blotted on polyvinylidene fluoride membranes (Millipore, USA) and probed with appropriated antibodies. The protein bands were developed with a chemiluminescence reagent (Bio-Rad, USA) and visualized with an ImageLab Scanner (Bio-Rad, USA).

Antibodies against HSV-1 ICP0, ICP8, and VP16 used here are described elsewhere. [24] Other antibodies used in this study included anti-STING (Cat.19851–1-AP, Proteintech, USA), anti-USP20 (Cat.17491-1-AP, Proteintech, USA), anti-USP18 (Cat.4813. Cell Signaling Technology, USA), anti-β-actin (60,008–1-Ig, Proteintech, USA), and anti-Ub (sc-8017, Santa Cruz Biotechnology, USA).

Co-IP assay

Cell lysates were harvested and Co-IP experiments were performed using the Dynabeads Antibody Coupling Kit following the manufacturer's instructions (Cat. 14311D; Life Technologies, USA). Rabbit IgG (Cat. 2729; Cell Signaling Technologies, USA) was used as the negative control for excluding unspecific binding. Immunoprecipitates were eluted by boiling with 1% (w/v) SDS sample buffers and analyzed with western blot assay.

Cell viability assay

Cells (3,000 per well) seeded in 96-well plates at 37°C for overnight incubation were treated with GSK2643943A, T1012G, and T1012G plus GSK2643943A. The viability of the cells was determined by CCK-8 Assays Kit (Cat.C0042, Beyotime) according to the manufacturer's instructions, and the OD_{450} was detected using the BioTek Epoch (BioTek Instruments, USA).

Animal test

The animal studies were done following guidelines and protocols approved by the Institutional Animal Care and Use Committee of the Shenzhen International Institute for Biomedical Research. For the subcutaneous xenograft model, SCC9 or SCC7 cells (8×10^6 cells or $1x10^6$ cells) were inoculated subcutaneously into the right flanks of 5-week-old female BALB/c nude mice or C3H/HeN mice, respectively. Once the tumor volume reached 70 to 120 mm^3, the mice were randomized into four groups (n = 6–7, per group) for indicated treatments as described in the main text. Tumor sizes were measured by length and width every 2 to 3 days and calculated based on the following formula: length × $width^2$ × 0.5.

Statistical analysis

The mean and SEM were used for the description of data variability. Statistical analyses were performed using two-tailed unpaired Student's t test for two independent group comparisons, while two-way ANOVA was used for more than two group comparisons by using SPSS software, and $^*p < 0.05$, $^{**}p < 0.01$, and $^{***}p < 0.001$ were considered statistically significant.

ACKNOWLEDGMENTS

This work was supported by grants from the Science, Technology and Innovation Commission of Shenzhen Municipality (CN) KCXFZ 202002011010232, Guangdong Basic and Applied Basic Research Foundation (CN) 2019A1515110069 to Shenzhen International Institute for Biomedical Research; the grants from Guangdong Nature Science Foundation 2016A030308007, Young Scientists Fund of National Natural Science Foundation of China 31900136 to Guangzhou Medical University.

AUTHOR CONTRIBUTIONS

R.T.L., G.G.Z., and W.M.F. conceived and designed the study. R.T.L., G.X.W., and M.L.C. performed the experiments and analyzed the data. W.M.F. interpreted the data and drafted the manuscript. G.G.Z. and W.M.F. reviewed the manuscript and supervised the study. R.T.L. and G.X.W. contributed equally.

DECLARATION OF INTERESTS

The authors declared that they have no conflicts of interest to this work.

REFERENCES

1. Ferlay, J., Soerjomataram, I., Dikshit, R., Eser, S., Mathers, C., Rebelo, M., Parkin, D.M., Forman, D., and Bray, F. (2015). Cancer incidence and mortality worldwide: sources, methods and major patterns in GLOBOCAN 2012. Int. J. Cancer *136*, E359–E386.

2. Warnakulasuriya, S. (2009). Global epidemiology of oral and oropharyngeal cancer. Oral Oncol. *45*, 309–316.

3. Coffin, R.S. (2016). Oncolytic immunotherapy: an emerging new modality for the treatment of cancer. Ann. Oncol. *27*, 1805–1808.

4. Wang, P.Y., Swain, H.M., Kunkler, A.L., Chen, C.Y., Hutzen, B.J., Arnold, M.A., Streby, K.A., Collins, M.H., Dipasquale, B., Stanek, J.R., et al. (2016). Neuroblastomas vary widely in their sensitivities to herpes simplex virotherapy unrelated to virus receptors and susceptibility. Gene Ther. *23*, 135–143.

5. Froechlich, G., Caiazza, C., Gentile, C., D'Alise, A.M., De Lucia, M., Langone, F., Leoni, G., Cotugno, G., Scisciola, V., Nicosia, A., et al. (2020). Integrity of the antiviral STING-mediated DNA sensing in tumor cells is required to sustain the immunotherapeutic efficacy of herpes simplex oncolytic virus. Cancers (Basel) *12*, 3407.

6. Dellac, S., Ben-Dov, H., Raanan, A., Saleem, H., Zamostiano, R., Semyatich, R., Lavi, S., Witz, I.P., Bacharach, E., and Ehrlich, M. (2020). Constitutive low expression of antiviral effectors sensitizes melanoma cells to a novel oncolytic virus. Int. J. Cancer. https://doi.org/10.1002/ijc.33401.

7. Kennedy, E.M., Farkaly, T., Grzesik, P., Lee, J., Denslow, A., Hewett, J., Bryant, J., Behara, P., Goshert, C., Wambua, D., et al. (2020). Design of an interferon-resistant oncolytic HSV-1 incorporating redundant safety modalities for improved tolerability. Mol. Ther. Oncolyt. *18*, 476–490.

8. Lee, J.M., Ghonime, M.G., and Cassady, K.A. (2019). STING restricts oHSV replication and spread in resistant MPNSTs but is dispensable for basal IFN-stimulated gene upregulation. Mol. Ther. Oncolytics *15*, 91–100.

9. Burke, S., Shergold, A., Elder, M.J., Whitworth, J., Cheng, X., Jin, H., Wilkinson, R.W., Harper, J., and Carroll, D.K. (2020). Oncolytic Newcastle disease virus activation of the innate immune response and priming of antitumor adaptive responses in vitro. Cancer Immunol. Immunother. *69*, 1015–1027.

10. Cui, J., Song, Y., Li, Y., Zhu, Q., Tan, P., Qin, Y., Wang, H.Y., and Wang, R.F. (2014). USP3 inhibits type I interferon signaling by deubiquitinating RIG-I-like receptors. Cell Res. *24*, 400–416.

11. Fan, Y., Mao, R., Yu, Y., Liu, S., Shi, Z., Cheng, J., Zhang, H., An, L., Zhao, Y., Xu, X., et al. (2014). USP21 negatively regulates antiviral response by acting as a RIG-I deubiquitinase. J. Exp. Med. *211*, 313–328.

12. Friedman, C.S., O'Donnell, M.A., Legarda-Addison, D., Ng, A., Cardenas, W.B., Yount, J.S., Moran, T.M., Basler, C.F., Komuro, A., Horvath, C.M., et al. (2008). The tumour suppressor CYLD is a negative regulator of RIG-I-mediated antiviral response. EMBO Rep. *9*, 930–936.

13. Zhang, M.X., Cai, Z., Zhang, M., Wang, X.M., Wang, Y., Zhao, F., Zhou, J., Luo, M.H., Zhu, Q., Xu, Z., et al. (2019). USP20 promotes cellular antiviral responses via deconjugating K48-linked ubiquitination of MITA. J. Immunol. *202*, 2397–2406.

14. Yan, R.Z.X., Chen, X., Liu, X., Tang, Y., Ma, J., Wang, L., et al. (2019). Enhancement of oncolytic activity of oHSV expressing IL-12 and anti PD-1 antibody by concurrent administration of exosomes carrying CTLA-4 miRNA. Immunotherapy *5*, 154–163.

15. Zong, Z.Z.Z., Wu, L., Zhang, L., and Zhou, F. (2020). The functional deubiquitinating enzymes in control of innate antiviral immunity. Adv. Sci. https://doi.org/10.1002/advs.202002484.

16. Tan, Y., Zhou, G., Wang, X., Chen, W., and Gao, H. (2018). USP18 promotes breast cancer growth by upregulating EGFR and activating the AKT/Skp2 pathway. Int. J. Oncol. *53*, 371–383.

17. Ishikawa, H., and Barber, G.N. (2008). STING is an endoplasmic reticulum adaptor that facilitates innate immune signalling. Nature *455*, 674–678.

18. Ishikawa, H., Ma, Z., and Barber, G.N. (2009). STING regulates intracellular DNA-mediated, type I interferon-dependent innate immunity. Nature *461*, 788–792.

19. Zhang, M., Zhang, M.X., Zhang, Q., Zhu, G.F., Yuan, L., Zhang, D.E., Zhu, Q., Yao, J., Shu, H.B., and Zhong, B. (2016). USP18 recruits USP20 to promote innate antiviral response through deubiquitinating STING/MITA. Cell Res *26*, 1302–1319.

20. Zhong, B., Yang, Y., Li, S., Wang, Y.Y., Li, Y., Diao, F., Lei, C., He, X., Zhang, L., Tien, P., and Shu, H.B. (2008). The adaptor protein MITA links virus-sensing receptors to IRF3 transcription factor activation. Immunity *29*, 538–550.

21. Wu, C., Luo, K., Zhao, F., Yin, P., Song, Y., Deng, M., Huang, J., Chen, Y., Li, L., Lee, S., et al. (2018). USP20 positively regulates tumorigenesis and chemoresistance through beta-catenin stabilization. Cell Death Differ. *25*, 1855–1869.

22. Duex, J.E., Comeau, L., Sorkin, A., Purow, B., and Kefas, B. (2011). Usp18 regulates epidermal growth factor (EGF) receptor expression and cancer cell survival via microRNA-7. J. Biol. Chem. *286*, 25377–25386.

23. Liu, Q., Wu, Y., Qin, Y., Hu, J., Xie, W., Qin, F.X., and Cui, J. (2018). Broad and diverse mechanisms used by deubiquitinase family members in regulating the type I interferon signaling pathway during antiviral responses. Sci. Adv. *4*, eaar2824.

24. Huang, R., Wu, J., Zhou, X., Jiang, H., Guoying Zhou, G., and Roizman, B. (2019). Herpes simplex virus 1 MicroRNA miR-H28 exported to uninfected cells in exosomes restricts cell-to-cell virus spread by inducing gamma interferon mRNA. J. Virol. *93*, e01005–e01019.